ResearchGate

See discussions, stats, and author profiles for this publication at: https://www.researchgate.net/publication/263046712

New Insight into Intermediate Precursors of Brust–Schiffrin Gold Nanoparticles Synthesis

ARTICLE *in* THE JOURNAL OF PHYSICAL CHEMISTRY C · MAY 2013

Impact Factor: 4.77 · DOI: 10.1021/jp402116x

CITATIONS
11

READS
79

8 AUTHORS, INCLUDING:

Chengchen Guo
Arizona State University
10 PUBLICATIONS **23** CITATIONS
SEE PROFILE

Xiaoliang Wang
Nanjing University
45 PUBLICATIONS **283** CITATIONS
SEE PROFILE

Pingchuan Sun
Nankai University
119 PUBLICATIONS **1,541** CITATIONS
SEE PROFILE

Wei Chen
Central South University
538 PUBLICATIONS **15,503** CITATIONS
SEE PROFILE

Available from: Chengchen Guo
Retrieved on: 26 January 2016

THE JOURNAL OF PHYSICAL CHEMISTRY C

Article

pubs.acs.org/JPCC

New Insight into Intermediate Precursors of Brust–Schiffrin Gold Nanoparticles Synthesis

Lili Zhu,[†] Chen Zhang,[†] Chengchen Guo,[†] Xiaoliang Wang,[†] Pingchuan Sun,[‡] Dongshan Zhou,[†] Wei Chen,[†] and Gi Xue*[,†]

[†]Department of Polymer Science and Engineering, School of Chemistry and Chemical Engineering, The State Key Laboratory of Coordination Chemistry, Nanjing University, 210093, People's Republic of China

[‡]Key Laboratory of Functional Polymer Materials, Ministry of Education, Nankai University, Tianjin 300071, People's Republic of China

Supporting Information

ABSTRACT: There is an ongoing intensive debate on the mechanism of gold nanoparticles formation regarding the intermediate precursors prior to the addition of reducing agent. A new detailed view of the widely used Brust–Schiffrin two-phase method to prepare gold nanoparticles is presented here. Precursor species of these reactions have been identified and quantified by NMR, UV–visible, Fourier-transform Raman spectroscopy, etc. We demonstrate that tetraalkylammonium gold complexes ([TOA][AuX_2]) and soluble gold thiolate ([TOA][AuSRX] and [TOA][$Au(SR)_2$]) were detectable as the precursors by NMR spectroscopy. Their relative contents depend on the concentration of reactants. Higher concentration of the reactants is favorable for the formation of soluble thiolate. Polymeric gold thiolate [Au(I)SR]$_n$ could eventually precipitate from the solution under specific conditions. The clear mechanism presented here is of great significance to tailor the size and properties of the final products.

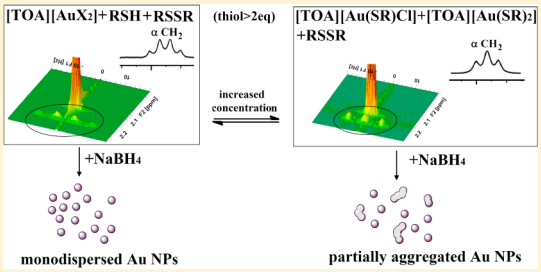

INTRODUCTION

The outstanding behaviors of gold nanoparticles (Au NPs) arise from their fascinating optical, electronic, catalytic, and chemical properties, which are intimately correlated with their size and the chemical nature of their core and surface species.[1−7] Wet chemistry techniques based on chemical reactions in solution are widely used to yield Au NPs with a wide range of sizes, shapes, and dielectric environments. Among them, the Brust–Schiffrin two-phase method is the most popular route to prepare organic ligands (mostly thiolate) stabilized Au NPs.[1] Since it was introduced, it has inspired a number of related approaches[7,8] and been successfully applied to synthesize other metal nanoparticles.[9,10] The kinetics for the NPs formation is very critical to generate uniform NPs with size control.[11−14] However, there remain significant questions regarding the detailed mechanism.[15−22] In particular, there is an ongoing debate regarding the precursor species prior to reduction.

Brust–Schiffrin two-phase synthesis generally consists of three steps: (i) hydrogen tetrachloroaurate ($HAuCl_4$) in water was transferred into the organic layer (i.e., toluene, chloroform, or benzene) by the phase transfer agent tetraoctylammonium bromide (TOAB); (ii) thiols were added to the organic phase and Au(III) was reduced to Au(I); and (iii) finally, 1−3 nm monodispersed Au NPs was synthesized by addition of the reducing agent sodium borohydride ($NaBH_4$). The early accepted assumption about this method by Schaaff, Murray et al. has been that polymeric Au(I) thiolate [Au(I)SR]$_n$ can be generated as intermediate precursors.[12−16] However, these proposed precursor species have been confirmed to be insoluble in common solvents and are very difficult to investigate in solution. Yet recently, research from Lennox[3] and Tong[4,23] has shown otherwise and draws the mechanistic studies into question. It was shown that [Au(I)SR]$_n$ was not a measurable (by ^{1}H NMR) precursor in reaction solution and tetraalkylammonium metal complex [TOA][AuX_2] was the relevant intermediate Au species. In spite of these reports, a limited number of studies have examined the mechanism. In general, the synthesis mechanism remains a major challenge and deserves further exploration. Investigating the composition of precursor species could also lead to clues on how to control the properties of resulting NPs, thus a particular focus is placed on the precursor of metal ions prior to the addition of reductant.

In the present study, we used 1-octadecanethiol ($C_{18}SH$) to undergo the Brust–Schiffrin two-phase reaction in toluene. We focused our investigations on the composition of the intermediate precursors after addition of thiols into Au^{3+} solution. Presursors before adding the reductant were in situ monitored by NMR spectroscopy (1D ^{1}H NMR, Homonuclear J-resolved 2D NMR, ^{1}H−^{1}H COSY). Tetraalkylammonium gold complexes ([TOA][AuX_2]) and soluble gold thiolate

Received: March 1, 2013
Revised: May 3, 2013
Published: May 6, 2013

 © 2013 American Chemical Society dx.doi.org/10.1021/jp402116x | J. Phys. Chem. C 2013, 117, 11399−11404

([TOA][AuSRX] and [TOA][Au(SR)$_2$]) were found to be detectable as the precursors by NMR spectroscopy. Polymeric [Au(I)SR]$_n$ could eventually precipitate from the solutions under radiation of normal laboratory light for long time, which indicates [Au(I)SR]$_n$ could not be counted as one of the intermediate precursors in the synthesis procedure. Finally, we experimentally verified that the clear mechanism presented here provides an effective synthetic strategy to obtain well-monodispersed nanoparticles by controlling the intermediate precursor.

EXPERIMENTAL METHODS

Materials. Tetraoctylammonium bromide (TOAB 98%), sodium borohydride ($NaBH_4$ 99%), hydrogen tetrachloroaurate ($HAuCl_4 \cdot 4H_2O$), and 1-octadecanethiol ($C_{18}SH$) were purchased from Sigma-Aldrich Co. Deuterated toluene was purchased from Alfa Aesar. All of the solvents were commercially available and distilled before use. All glassware was cleaned with aqua regia (HCl:HNO_3= 3:1 vol %) and rinsed with copious amounts of nanopure water, then dried in an oven prior to use.

Sample Preparation. The gold complex with TOAB during the reaction was prepared by a typical two-phase Brust–Schiffrin method.[1,3] An aqueous solution of $HAuCl_4 \cdot 4H_2O$ (70 mg in 10 mL, 1 equiv) was mixed with a solution of TOAB in *d*-toluene (233 mg in 10 mL, 2.5 equiv). This concentration was used as a typical one (C_0).[3] The two-phase mixture was rapidly stirred until Au^{3+} was all transferred to the organic phase to give a wine-red solution. The [TOA][AuX_4] was produced with a mix of Cl^- and Br^- ions. After discarding the aqueous phase, the [TOA][AuX_4] complex solution in the organic phase was then transferred to a new reaction vessel for further reaction. $C_{18}SH$ (0, 1, 2, 3, or 4 equiv relative to the Au in each aliquot) was added to each of five equal aliquots of *d*-toluene solution with the same concentration (C_0). Each sample was stirred for about 2 h.

Water may have great impact on the structures of intermediates. It has been proved that large quantities of water could accelerate the formation of white precipitate while small amounts of water do not lead to measurable quantities of [Au(I)SR]$_n$.[3] In our experiments the water phase was carefully removed. The experimental process was exactly the same as the typical two-phase synthesis, thus the NMR experiment truly reflected the real synthesis procedure.

Instruments. Surface enhanced Raman scattering (SERS) experiments were performed on a Bruker MultiRAM with a 1064 nm Nd:YAG laser source and Ge detector. The spectra were collected with laser power of 10 mw and scan times of 400 if not specified.

Transmission electron microscopy (TEM) images were recorded by using a JEOL JEM-2100 electron microscope at an accelerating bias voltage of 200 kV. A drop of dilute solution containing Au NPs was deposited on a copper grid. The solvent was allowed to evaporate under atmospheric conditions.

1D ^{1}H NMR spectra and 2D J-resolved NMR were obtained on an AV-400 NMR spectrometer (Bruker BioSpin, Coventy, UK), equipped with a 5 mm PABBO BB probe, and operated at 400.13 MHz with a sample temperature of 25 °C.

1D ^{1}H NMR spectra were obtained by using a 30° excitation pulse, 8 kHz spectral width, and 5 s relaxation delay. Eight transients were acquired by using 400k data points resulting in a 5 min total acquisition time per 1D spectrum. The resulting data were then Fourier transformed, manually phase corrected, and calibrated, all using TopSpin (version 3.0; Bruker).

2D J-resolved NMR spectra were acquired by using 16 transients per increment for 32 increments that were collected into 32k data points and zero filled to 32k data points prior to 2D Fourier transformation. The spectral width was 4 kHz in the direct dimension (F2) and 50 Hz in the indirect dimension (F1), giving a digital resolution of 0.39 Hz in Fl and 2.01 Hz in F2. Next the 2D spectra were tilted and, if required, symmetrized and calibrated, all using TopSpin (version 3.0; Bruker).

^{1}H–^{1}H COSY spectra of extracts were obtained on a DRX-500 NMR spectrometer (Bruker BioSpin, Coventy, UK) by summing 8 for each of 128 increments in *t*, acquired as a matrix of 130k data points in the time domain, and zero filled to130k data points prior to 2D Fourier transformation. The spectral width was 5 kHz along both F2 and Fl, and the resulting digital resolution was 4.88 Hz in the F2 dimensions and 25.38 Hz in the F2 dimensions. Finally, the spectra were processed by using TopSpin (version 3.0; Bruker).

^{1}H solid state NMR (SSNMR) experiments were performed on a Varian Infinityplus-400 wide-bore (89 mm) NMR spectrometer at a proton frequency of 399.7 MHz. A 2.5 mm T3 double-resonance CPMAS probe was used for ^{1}H SSNMR experiments, and it can provide stable spinning up to 30 kHz within ±2 Hz with use of a zirconia PENCIL rotor. The magic angle spinning (MAS) frequency used in our experiments was 25 kHz. The ^{1}H chemical shifts were referenced to external TMS. The 90° pulse width was 1.4 μs. Recycle delays between two scans were set to 6 s. The spectra were obtained with 32 scans for each spectrum. The background signal was separately collected under the same condition without sample and then subtracted from the spectra acquired with a sample to obtain all of the spectra used in the subsequent analysis. All of the NMR data were processed with Varian Spinsight software, and all experiments were carried out at room temperature.

RESULTS AND DISCUSSION

Complete reduction from Au(III) to Au(I) occurred with the addition of 2 equiv of thiols, as shown by UV–visible absorption spectra in Figure S1. We monitored the splitting of αCH_2 peaks in the NMR spectrum caused by J-coupling for $C_{18}SH$ in solution. Figure 1 shows ^{1}H NMR spectra recorded

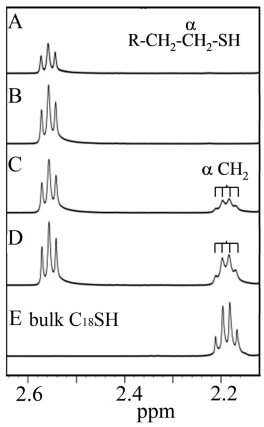

Figure 1. ^{1}H NMR spectra of TOAX + [TOA][AuX_4] solution in *d*-toluene at concentration C_0 with (A) 1, (B) 2, (C) 3, and (D) 4 equiv of $C_{18}SH$ added and (E) bulk $C_{18}SH$.

dx.doi.org/10.1021/jp402116x | J. Phys. Chem. C 2013, 117, 11399–11404

for the Brust−Schiffrin two-phase reaction in *d*-toluene with different equivalents of $C_{18}SH$ added to TOAX + [TOA]-[AuX_4] solution at concentration C_0. For disulfides and free thiols, triplet and quartet peaks were observed, respectively. For thiolate, the αCH_2 peak was a triplet. After the addition of 1 and 2 equiv of $C_{18}SH$, octadecyl disulfide was generated through complete oxidation of the added thiol, as shown by the triplet at ca. 2.55 ppm (Figure 1A,B). Addition of 3 and 4 equiv of $C_{18}SH$, respectively, resulted in quartet NMR peaks (αCH_2 at ca. 2.2 ppm) in *d*-toluene, indicating that free thiol was generated in NMR measurable quantities.

We changed the concentration of the reactants and found significant differences in the detected precursors. After addition of 3 equiv of $C_{18}SH$ to TOAX + [TOA][AuX_4] *d*-toluene with varied concentrations, NMR spectra of the intermediate precursors were recorded in Figure 2. The quartet peak

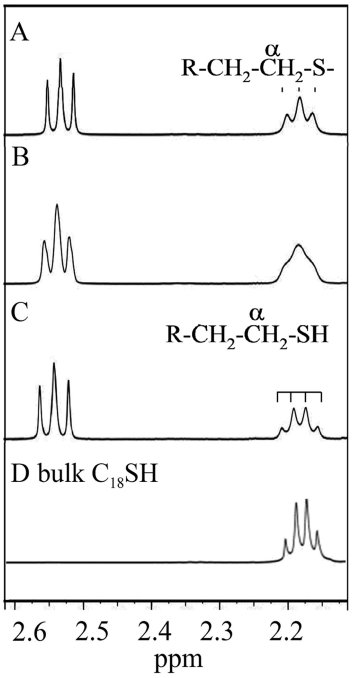

Figure 2. ^1H NMR spectra of TOAX + [TOA][AuX_4] solution in *d*-toluene with 3 equiv of $C_{18}SH$ added at concentrations of (A) $5C_0$, (B) $3C_0$, (C) C_0, and (D) bulk $C_{18}SH$.

(αCH_2 at ca. 2.2 ppm) in Figure 2C indicates the excess free thiol in the solution at C_0. As the concentration increases to $5C_0$, the NMR peak changes to triplet (Figure 2A), indicating the generation of soluble thiolate at concentrated solution. The NMR investigation clearly indicates that thiolate is not generated in dilute solution in NMR measurable amount, and that a higher concentration is favorable for dissociation of thiol to generate thiolate. The concentration effect on the dissociation of thiols is probably due to two factors: the increase in polarity and the reduction in acidity of the entire solution at high concentration of reactants (including TOAB). It is noteworthy that this is the first in situ experimental observation of soluble thiolate during two-phase synthesis of Au NPs by ^1H NMR spectroscopy.

Indistinct broad peaks in the 1D ^1H NMR spectrum (shown in Figure 2B) for intermediates containing both free thiol and soluble thiolate are further confirmed by Homonuclear J-resolved 2D spectrum (HOM2DJ). By using the technique of complete homonuclear decoupling in a H-nuclear magnetic resonance, we can obtain a spectrum with better signal resolution and chemical shift determinations. HOM2DJ[24] would accomplish complete homonuclear decoupling while retaining all coupling information. After 3 equiv of $C_{18}SH$ is added in a solution of [TOAB][AuX_4], αCH_2 shows a quartet with concentration C_0 (Figure 3A) and a triplet with

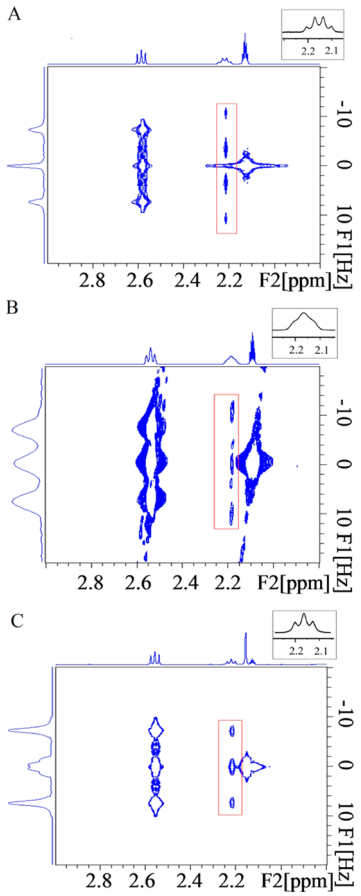

Figure 3. Homonuclear J-resolved 2D spectrum of TOAX + [TOA][AuX_4] solution with 3 equiv of $C_{18}SH$ added in *d*-toluene at changing concentration: (A) C_0; (B) $3C_0$, and (C) $5C_0$. In this figure, axis F2 shows the proton chemical shift, and F1 shows the separation of the component lines of each multiplet. Insert: Corresponding 1D ^1H NMR spectra.

concentration $5C_0$ (Figure 3C). According to the chemical shift, the peaks of αCH_2 with $3C_0$ (Figure 3B) can be resolved into a group of triplets (signal from thiolate) and a group of quartets (signal from thiol). Figure 3 also indicates that the αCH_2 peak at about ca. 2.2 ppm in *d*-toluene changes from quartet to triplet with increased concentration. The HOM2DJ spectrum can give more information of reaction products when peaks appear as a broadened singlet in a 1-D ^1H NMR spectrum.

Further $^1H-^1H$ COSY spectroscopy experiments give correlation signals that correspond to pairs of hydrogen atoms which are connected through chemical bonds. $^1H-^1H$ COSY is a useful method for determining which signals arise from neighboring protons. Figure 4A shows the H−H coupling information of bulk C_{18}−SH in *d*-toluene, the cross peaks (inside the circle) indicate the existence of three-bond H−H coupling αCH_2-βCH_2 and αCH_2−SH. These cross peaks can

dx.doi.org/10.1021/jp402116x | *J. Phys. Chem. C* 2013, 117, 11399−11404

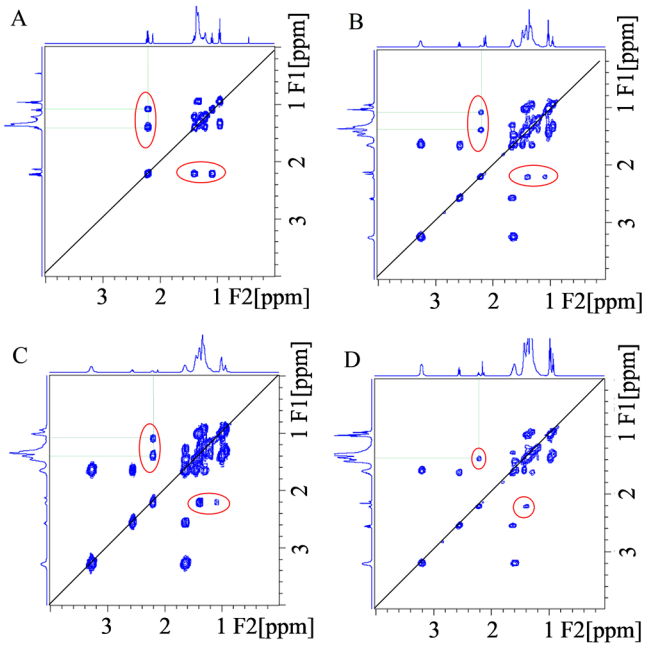

Figure 4. The ^{1}H−^{1}H COSY spectrum in *d*-toluene (A) and solutions of bulk $C_{18}SH$ (B−D), TOAX + [TOA][AuX_4] solution with 3 equiv of $C_{18}SH$ added at different solution concentrations: (B) C_0, (C) $3C_0$, and (D) $5C_0$.

also be observed in panels B and C of Figure 4, which indicates the existence of free thiol. However, the cross peak due to coupling between αCH_2 and SH disappears when the solution concentration increases to $5C_0$ (Figure 4D). This means almost all of the third equivalent of thiol has reacted with [TOA][AuX_2] and forms thiolate at $5C_0$. On the other hand, these two cross peaks have nearly the same intensity in panels A and B of Figure 4. Nevertheless, in Figure 4C, the cross peak due to the correlation between αCH_2 and SH is much weaker than when the cross peak involves αCH_2 and βCH_2, which suggests that only a part of the third equivalent of thiol is involved in the formation of Au(I) thiolate with the remaning thiol existing in free state when the solution concentration increases from C_0 to $3C_0$

During the experiment, precipitates did not show up in the initial stage even at the presence of NMR triplet peaks for thiolate. After the reaction vessels were left in the laboratory for some days, white precipitates gradually appeared. These precipitates were characterized to be $[Au(I)SR]_n$ by Raman and ^{1}H SSNMR (Figure 5). Comparing Raman spectra in Figure 5A to 5B (left), it is found that the S−H vibration at 2569 cm^{-1} disappears and a new peak at 309 cm^{-1} assigned to Au−S appears. This result suggests that the $[Au(I)SC_{18}H_{37}]_n$ is very likely formed after 4 equiv of $C_{18}SH$ has been added for several days. As shown in Figure 5, right, in ^{1}H SSNMR spectra the peaks at 1.2 and 0.8 ppm are assigned to methylene and methyl protons, respectively. The precipitation speed depends on the concentration of the reactants, thiol structures, surrounding environments, etc.[17,25−28] According to our observations, $[Au(I)SC_{18}H_{37}]_n$ seems to precipitate more quickly in concentrated solutions. We changed the amount of TOAB; when 1equiv or 4 equiv of TOAB was added to the solution, white precipitate could not be found 2−3 days later, which indicated $[Au(I)SR]_n$ did not form. $[Au(I)SR]_n$ could transform into surfactant-free gold nanoparticles under special conditions, such as under the heat treatment process.[29,30] In

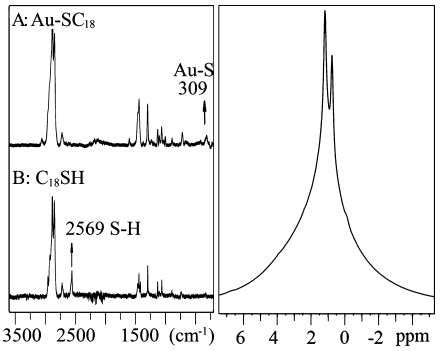

Figure 5. (Left) Raman spectra of (A) white precipitate from TOAX + [TOA][AuX_4] solution with 4 equiv of $C_{18}SH$ and (B) bulk $C_{18}SH$. (Right): ^{1}H SSNMR spectra of the precipitate.

real synthesis, after the addition of thiols $NaBH_4$ an aqueous solution was added 10−30 min later. The solution was homogeneous without precipitate when reducing agent was added. Therefore, insoluble polymeric $[Au(I)SR]_n$ could not be counted as one of the intermediate precursors in the synthesis procedure.

The change of precursor solution during precipitation was further followed by ^{1}H NMR spectroscopy, as shown in Figure 6. Figure 6A shows a triplet peak at ca. 2.2 ppm due to αCH_2 of

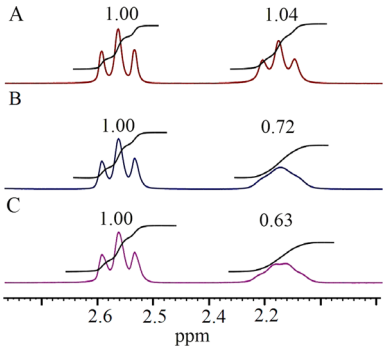

Figure 6. ^{1}H NMR spectra of TOAX + [TOA][AuX_4] solution in *d*-toluene with 4 equiv of $C_{18}SH$ added at $5C_0$: (A) the initial mixed solution; (B) the solution held for 7 days, and (C) the solution held for 15 days. We normalized the integral of the proton peak for disulfide as 1. The relative intensity for peaks at ca. 2.2 ppm is indicated on each curve.

$C_{18}S$-, indicating the existence of soluble thiolate after addition of the thiol into [TOA][AuX_4] complex solution. We monitored the signal changes as compared with that for octadecyl disulfide at ca. 2.55 ppm. The spectrum for the initial mixture (Figure 6A) shows that the ratio of signal integration is nearly 1:1. After precipitation, the intensity of the 2.2 ppm peak reduces gradually. The integration ratio changes to 1:0.63 after precipitation proceeded for 15 days. Interestingly, the peak shape changed from triplet to more pronounced quartet, confirming that $C_{18}SH$ was initially dissociated (Figure 6A) and then reformed again (Figure 6C) after precipitation of $[Au(I)SR]_n$.

On the basis of the above NMR spectroscopic studies, we found several species could exist as the intermediate precursors for the two-phase Brust−Schiffrin reaction. All these species could be reduced to Au NPs after addition of $NaBH_4$. If large amounts of soluble thiolate existed in measurable quantity, such as in toluene with 5 equiv of $C_{18}SH$ added at $5C_0$, the reduced

dx.doi.org/10.1021/jp402116x | J. Phys. Chem. C 2013, 117, 11399−11404

particles were not uniform and partially aggregated (shown in Figure S2). It has already been reported that partial metal(I) thiolate formation generates unknown mixtures of multiple metal precursors and produces mixed layers on the NPs.[28,31−33] Our result experimentally verified the expectation that in some cases substantial amounts of detectable soluble thiolate complexes in solutions may lead to poor synthetic outcomes in two-phase reaction.[3]

CONCLUSIONS

In summary, an overall view of the Brust−Schiffrin two-phase method mechanism has been detailed here. Precursor species have been identified and quantified. The result indicates that increased concentration is beneficial for the formation of soluble thiolate complexes while $[TOA][AuX_2]$ complex forms in dilute solutions. We demonstrate that the synthesis procedure could undergo two pathways regulated by reactant concentration (Scheme 1). Pathway A, which leads to intermediates containing free thiol and $[TOA][AuX_2]$, is favored by low concentration. Pathway B leads to precursors consisting of soluble thiolate species at high concentration. The precursor medium that contains mainly $[TOA][AuX_2]$ complex and excess thiol can be reduced to well-monodispersed small Au nanoparticles. However, the existence of large amounts of soluble thiolate species in solution seems not to favor the formation of small and uniform particles in the Brust−Schiffrin two-phase reaction.

Scheme 1. Proposed Mechanism for the Brust−Schiffrin Two-Phase Gold Nanoparticles Synthesis

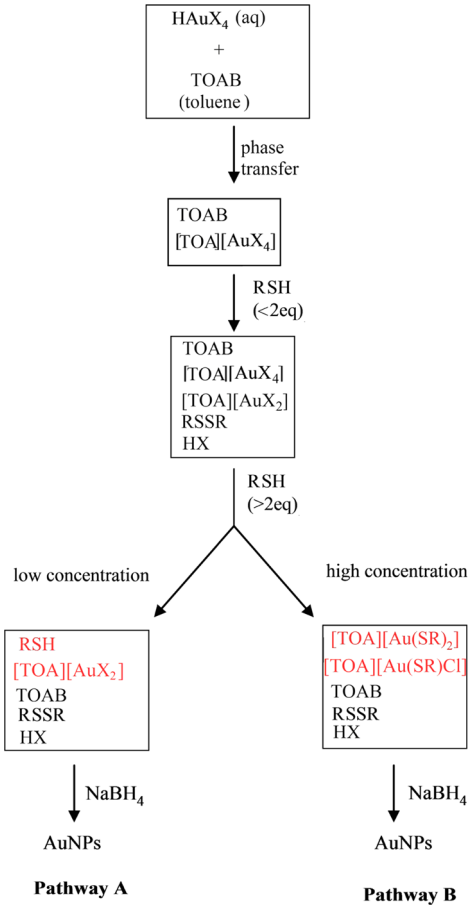

ASSOCIATED CONTENT

Supporting Information

UV−visible and TEM characterization mentioned in the paper. This material is available free of charge via the Internet at http://pubs.acs.org.

AUTHOR INFORMATION

Corresponding Author

*Tel: +86 25-83686136. Fax: 86-25-83317761. E-mail: xuegi@nju.edu.cn.

Notes

The authors declare no competing financial interest.

ACKNOWLEDGMENTS

We gratefully acknowledge National Basic Research Program of China (973 Program, 2012 CB 821503) and the support from the National Science Foundation of China (Nos. 51133002, 21174062, 21274060, 21274059, and 21074052).

REFERENCES

(1) Brust, M.; Walker, M.; Bethell, D.; Schiffrin, D. J.; Whyman, R. Synthesis of Thiol-Derivatized Gold Nanoparticles in a Two-Phase Liquid-Liquid System. *J. Chem. Soc., Chem. Commun.* **1994**, 801−802.

(2) Murray, R. W. Nanoelectrochemistry: Metal Nanoparticles, Nanoelectrodes, and Nanopores. *Chem. Rev.* **2008**, *108*, 2688−2720.

(3) Goulet, P. J. G.; Lennox, R. B. New Insights into Brust-Schiffrin Metal Nanoparticle Synthesis. *J. Am. Chem. Soc.* **2010**, *132*, 9582−9584.

(4) Li, Y.; Zaluzhna, O.; Zangmeister, C. D.; Allison, T. C.; Tong, Y. Y. J. Different Mechanisms Govern the Two-Phase Brust-Schiffrin Dialkylditelluride Synthesis of Ag and Au Nanoparticles. *J. Am. Chem. Soc.* **2012**, *134*, 1990−1992.

(5) Barngrover, B. M.; Aikens, C. M. Electron and Hydride Addition to Gold(I) Thiolate Oligomers: Implications for Gold-Thiolate Nanoparticle Growth Mechanisms. *J. Phys. Chem. Lett.* **2011**, *2*, 990−994.

(6) Zhu, L. L.; Wang, X. L.; Gu, Q.; Chen, W.; Sun, P. C.; Xue, G. Confinement-Induced Deviation of Chain Mobility and Glass Transition Temperature for Polystyrene/Au Nanoparticles. *Macromolecules* **2013**, *46*, 2292−2297.

(7) Sardar, R.; Funston, A. M.; Mulvaney, P.; Murray, R. W. Gold Nanoparticles: Past, Present, and Future. *Langmuir* **2009**, *25*, 13840−13851.

(8) Daniel, M. C.; Astruc, D. Gold Nanoparticles: Assembly, Supramolecular Chemistry, Quantum-Size-Related Properties, and Applications Toward Biology, Catalysis, and Nanotechnology. *Chem. Rev.* **2004**, *104*, 293−346.

(9) Murthy, S.; Bigioni, T. P.; Wang, Z. L.; Khoury, J. T.; Whetten, R. L. Liquid-phase Synthesis of Thiol-Derivatized Silver Nanocrystals. *Mater. Lett.* **1997**, *30*, 321−325.

(10) Kang, S. Y.; Kim, K. Comparative Study of Dodecanethiol-Derivatized Silver Nanoparticles Prepared in One-Phase and Two-Phase Systems. *Langmuir* **1998**, *14*, 226−230.

(11) Pei, Y.; Pal, R.; Liu, C. Y.; Gao, Y.; Zhang, Z. H.; Zeng, X. C. Interlocked Catenane-Like Structure Predicted in Au-24(SR)(20): Implication to Structural Evolution of Thiolated Gold Clusters from Homoleptic Gold(I) Thiolates to Core-Stacked Nanoparticles. *J. Am. Chem. Soc.* **2012**, *134*, 3015−3024.

(12) Brinas, R. P.; Hu, M. H.; Qian, L. P.; Lymar, E. S.; Hainfeld, J. F. Gold Nanoparticle Size Controlled by Polymeric Au(I) Thiolate Precursor Size. *J. Am. Chem. Soc.* **2008**, *130*, 975−982.

(13) Zhu, M.; Lanni, E.; Garg, N.; Bier, M. E.; Jin, R. Kinetically Controlled, High-Yield Synthesis of Au-25 Clusters. *J. Am. Chem. Soc.* **2008**, *130*, 1138−1139.

(14) Negishi, Y.; Nobusada, K.; Tsukuda, T. Glutathione-Protected Gold Clusters Revisited: Bridging the Gap Between Gold(I)-Thiolate

Complexes and Thiolate-Protected Gold Nanocrystals. *J. Am. Chem. Soc.* **2005**, *127*, 5261−5270.
(15) Schaaff, T. G.; Shafigullin, M. N.; Khoury, J. T.; Vezmar, I.; Whetten, R. L.; Cullen, W. G.; First, P. N.; GutierrezWing, C.; Ascensio, J.; JoseYacaman, M. J. Isolation of Smaller Nanocrystal Au Molecules: Robust Quantum Effects in Optical Spectra. *J. Phys. Chem. B* **1997**, *101*, 7885−7891.
(16) Jin, R. C. Quantum Sized, Thiolate-Protected Gold Nanoclusters. *Nanoscale* **2010**, *2*, 343−362.
(17) Barngrover, B. M.; Aikens, C. M. The Golden Pathway to Thiolate-Stabilized Nanoparticles: Following the Formation of Gold-(I) Thiolate from Gold(III) Chloride. *J. Am. Chem. Soc.* **2012**, *134*, 12590−12595.
(18) Ji, W.; Spegazzini, N.; Kitahama, Y.; Chen, Y. J.; Zhao, B.; Ozaki, Y. pH-Response Mechanism of p-Aminobenzenethiol on Ag Nanoparticles Revealed By Two-Dimensional Correlation Surface-Enhanced Raman Scattering Spectroscopy. *J. Phys. Chem. Lett.* **2012**, *3*, 3204−3209.
(19) Li, Y.; Zaluzhna, O.; Tong, Y. Y. J. Critical Role of Water and the Structure of Inverse Micelles in the Brust-Schiffrin Synthesis of Metal Nanoparticles. *Langmuir* **2011**, *27*, 7366−7370.
(20) Man, R. W. Y.; Brown, A. R. C.; Wolf, M. O. Mechanism of Formation of Palladium Nanoparticles: Lewis Base Assisted, Low-Temperature Preparation of Monodisperse Nanoparticles. *Angew. Chem., Int. Ed.* **2012**, *51*, 11350−11353.
(21) Corthey, G.; Rubert, A. A.; Picone, A. L.; Casillas, G.; Giovanetti, L. J.; Ramallo-Lopez, J. M.; Zelaya, E.; Benitez, G. A.; Requejo, F. G.; Jose-Yacaman, M.; et al. New Insights Into the Chemistry of Thiolate-Protected Palladium Nanoparticles. *J. Phys. Chem. C* **2012**, *116*, 9830−9837.
(22) Zaluzhna, O.; Li, Y.; Zangmeister, C.; Allison, T. C.; Tong, Y. J. Mechanistic Insights on One-Phase vs. Two-Phase Brust-Schiffrin Method Synthesis of Au Nanoparticles with Dioctyl-diselenides. *Chem. Commun.* **2012**, *48*, 362−364.
(23) Li, Y.; Zaluzhna, O.; Xu, B. L.; Gao, Y. A.; Modest, J. M.; Tong, Y. J. Mechanistic Insights into the Brust-Shiffrin Two-Phase Synthesis of Organo-Chalcogenate-Protected Metal Nanoparticles. *J. Am. Chem. Soc.* **2011**, *133*, 2092−2095.
(24) Aue, W. P.; Karhan, J.; Ernst, R. R. Homonuclear Broad-Band Decoupling and 2-Dimensional J-resolved NMR-Spectroscopy. *J. Chem. Phys.* **1976**, *64*, 4226−4227.
(25) Eller, P. G.; Kubas, G. J. Sulfur-dioxide Adducts of Organophosphinecopper(I) Mercaptide, Phenoxide, and Selenolate Complexes Coordinated SR-, OR-, and SER- as Lewis-Bases. *J. Am. Chem. Soc.* **1977**, *99*, 4346−4351.
(26) Voicu, R.; Badia, A.; Morin, F.; Lennox, R. B.; Ellis, T. H. Thermal Behavior of a Self-Assembled Silver n-Dodecanethiolate Layered Material Monitored by DSC, FTIR, and C-13 NMR Spectroscopy. *Chem. Mater.* **2000**, *12*, 2646−2652.
(27) Cha, S. H.; Kim, J. U.; Kim, K. H.; Lee, J. C. Preparation and Photoluminescent Properties of Gold(I)-Alkanethiolate Complexes Having Highly Ordered Supramolecular Structures. *Chem. Mater.* **2007**, *19*, 6297−6303.
(28) Wu, Z.; Suhan, J.; Jin, R. C. One-Pot Synthesis of Atomically Monodisperse, Thiol-Functionalized Au-25 Nanoclusters. *J. Mater. Chem.* **2009**, *19*, 622−626.
(29) Nakamoto, M.; Yamamoto, M.; Fukusumi, M. Thermolysis of Gold(I) Thiolate Complexes Producing Novel Gold Nanoparticles Passivated by Alkyl groups. *Chem. Commun.* **2002**, 1622−1623.
(30) Cha, S. H.; Kim, K. H.; Kim, J. U.; Lee, W. K.; Lee, J. C. Thermal Behavior of Gold(I)-Thiolate Complexes and Their Transformation Into Gold Nanoparticles Under Heat Treatment Process. *J. Phy. Chem. C* **2008**, *112*, 13862−13868.
(31) Donkers, R. L.; Lee, D.; Murray, R. W. Synthesis and Isolation of The Molecule-Like Cluster $Au_{38}(PhCH_2CH_2S)_{24}$. *Langmuir* **2004**, *20*, 1945−1952.
(32) Reilly, S. A.; Krick, T.; Dass, A. Surfactant-Free Synthesis of Ultrasmall Gold Nanoclusters. *J. Phys. Chem. C* **2010**, *114*, 741−745.
(33) Templeton, A. C.; Chen, S. W.; Gross, S. M.; Murray, R. W. Water-Soluble, Isolable Gold Clusters Protected by Tiopronin and Coenzyme A Monolayers. *Langmuir* **1999**, *15*, 66−76.